N96-18084

513-34
7335

P-10

Methods for Prismatic/Tetrahedral Grid Generation and Adaptation

Y. Kallinderis *

Dept. of Aerospace Engineering and Engineering Mechanics
The University of Texas at Austin
Austin, TX 78712

Abstract

The present work involves generation of hybrid prismatic/tetrahedral grids for complex 3-D geometries including multi-body domains. The prisms cover the region close to each body's surface, while tetrahedra are created elsewhere [8]. Two developments are presented for hybrid grid generation around complex 3-D geometries. The first is a new octree/advancing front type of method for generation of the tetrahedra of the hybrid mesh. The main feature of the present advancing front tetrahedra generator that is different from previous such methods is that it does not require the creation of a background mesh by the user for the determination of the grid-spacing and stretching parameters. These are determined via an automatically generated octree. The second development is a method for treating the narrow gaps in between different bodies in a multiply-connected domain. This method is applied to a two-element wing case. A High Speed Civil Transport (HSCT) type of aircraft geometry is considered. The generated hybrid grid required only 170 K tetrahedra instead of an estimated two million had a tetrahedral mesh been used in the prisms region as well. A solution adaptive scheme for viscous computations on hybrid grids is also presented [2]. A hybrid grid adaptation scheme that employs both h-refinement and redistribution strategies is developed to provide optimum meshes for viscous flow computations. Grid refinement is a dual adaptation scheme that couples 3-D, isotropic division of tetrahedra and 2-D, directional division of prisms.

An Octree/Advancing Front Method for Tetrahedra Generation

A new method is presented for generating the tetrahedra of the hybrid grid. Advancing front type of methods require specification by the user of the distribution of three parameters over the entire domain to be gridded. These field functions are: (i) the node spacing, (ii) the grid stretching,

*Associate Professor

and (iii) the direction of the stretching. In the present work these parameters do not need to be specified. The distribution of grid size, stretching, and direction of stretching is automatically determined via an octree. There is no need for a special background mesh which has been the backbone of previous advancing front generators.

The tetrahedra that are generated should progressively become larger as the front advances away from the original surface. Their size, the rate of increase of their size, as well as the direction of the increase are given from an octree consisting of cubes which is generated automatically via a *Divide-and-Conquer* method. This process generates octants that are progressively larger with distance away from the body. Their size will be the characteristic size of the tetrahedra that will be generated in their vicinity.

Generation starts from the outermost surface of the layer of prisms surrounding the body. The triangles of this surface form the initial front. Then, a list of points is created that consists of a new node, as well as of "nearby" existing points of the front. One of these points is chosen to connect to the vertices of the face. Following choice of the point to connect to, a new tetrahedron is formed. The list of the faces, edges, and points of the front is updated by adding and/or removing elements. The algorithm followed in the present work is the one presented in [3, 4]. The method requires a data structure which allows for efficient addition/removal of faces, edges and points, as well as for fast identification of faces and edges that intersect a certain region. The alternating digital tree (ADT) algorithm is employed for these tasks [5].

Figure 1 illustrates the symmetry plane of the HSCT geometry. The quadrilaterals (dark lines) correspond to the faces of the octants on this plane, while the triangles (light lines) correspond to the faces of the tetrahedra. It is observed that the size of the tetrahedra, as well the stretching of the mesh and the direction of stretching is guided quite accurately by the octree.

Simplicity and no user intervention are main advantages of the octree. The usual trial-and-error procedures for constructing the field functions that give the local size of the tetrahedra, the stretching of the mesh, and the direction of the stretching (background mesh) for previous advancing front generators are avoided in the present method. The octree is generated once and remains the same throughout the generation process. Details of the octree are presented in [7, 8].

Hybrid Grid Generation for Multi-Body Domains

The developed hybrid grid generation method is flexible and general in order to treat domains that contain multiple bodies. A prismatic layer is created around each one of the bodies, while the regions in between these meshes are filled with tetrahedra. Any location and orientation of these bodies is allowed. This is accomplished via a special method for treatment of narrow gaps that frequently form in multiply-connected domains, such as multi-element wings. The key feature of the method is the fact that the prismatic grid around each of the bodies is generated independently of all the other bodies. As a result, such generation is as simple as the generation of prisms for a domain containing a single body. However, overlapping meshes are avoided here by employing a special technique that redistributes the prisms nodes along their corresponding marching lines after the initial generation. This redistribution occurs in the vicinity of the regions of overlapping prismatic meshes and results in formation of gaps in between the previously overlapping prisms layers. Then a tetrahedral grid is generated in order to fill in those gaps. It should be emphasized

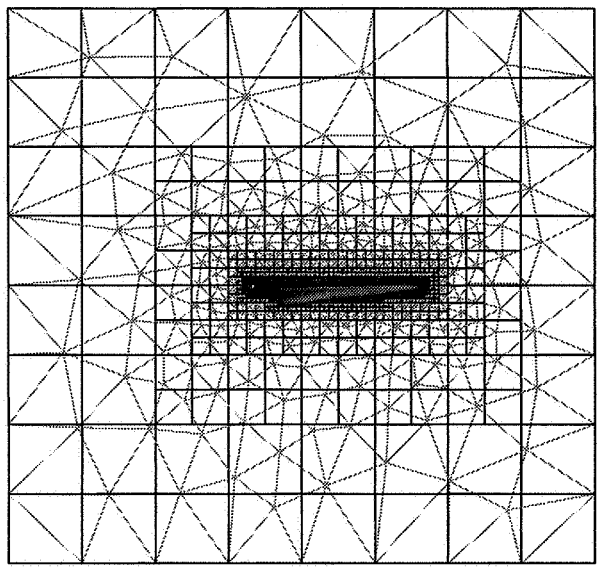

Figure 1: Effect of the octree on growth of the tetrahedra. View of the octants (quadrilateral faces), as well as of the tetrahedra (triangular faces) on the symmetry plane. Growth of the tetrahedra away from the outermost prisms surface follows growth of the octree quite faithfully.

that the structure of the prismatic grid is not destroyed. Further details of the method are given in [8].

In order to illustrate validity of the previous procedure, the case of a two-element wing with variable size of the gap between the main wing and its flap is considered. Stage one involves generation of the two separate prismatic meshes that cover each one of the two bodies. Generation is quite simple due to the fact that each layer of prisms is grown independently of the other layer. The two grids overlap locally as shown in Figure 2(a). In the second stage, the thickness of the prisms layers is reduced locally and the overlap no longer occurs as shown in Figure 2(b). Comparing the grids of Figure 2, it is observed that the receding occurs over a larger region which results in a smooth variation of the local thicknesses of both meshes. The final stage involves generation of the tetrahedral mesh that covers all areas in between the prisms. Figure 3 shows the final hybrid (prismatic/tetrahedral) grid on the plane of symmetry. The quadrilaterals are the signature of the prisms on that plane, while the triangles correspond to faces of the tetrahedral mesh.

Hybrid Grid for the HSCT

A High Speed Civil Transport (HSCT)-type of aircraft geometry was chosen as the test case for the developed grid generator. Figure 4 shows the triangulation of the initial surface. The mesh

consists of 4412 triangles and 2275 nodes. A symmetry plane is considered that divides the body. Thus, hybrid grid is generated for half of the space.

The time required to generate the prismatic grid around the HSCT was 90 seconds for 40 layers of prisms on an IBM 390 workstation. Generation of approximately 170,000 tetrahedra took about 67 minutes on the same station. It should be emphasized that employment of a hybrid grid for the HSCT geometry required only 170 K tetrahedra instead of an estimated two million had a tetrahedral mesh been used in the prisms region, as well.

Figure 5 illustrates the hybrid mesh on two different planes that are perpendicular to each other. The first plane is the symmetry and it is indicated by the darker lines, while the second is intersecting the fuselage at a location upstream of the wing and it is shown via light lines. It should be noted that the irregularity of the lines observed on the second plane are due to the fact that the grid it intersects is not planar as it is on the symmetry plane.

Combined Refinement/Redistribution for the Hybrid Grid

A dynamic grid adaptation algorithm has previously been developed for 3-D unstructured grids [6]. The algorithm is capable of simultaneously un-refining and refining appropriate regions of the flow domain. This method is extended to the present work and is coupled with prismatic grid adaptation to implement a hybrid adaptation method.

Directional Division of Prisms

The prisms are refined directionally in order to preserve the structure of the mesh along the normal-to-surface direction. The prismatic grid refinement proceeds by dividing only the *lateral* edges that lie on the wall surface and hence the wall faces. The faces are divided either into two or four subfaces. The resulting surface triangulation is replicated in each successive layer of the prismatic grid. This results in all the prisms that belong to the same stack (namely, the group of cells that originate from the same triangular face on the wall surface) getting divided alike. The prismatic grid refinement preserves the structure of the initial grid in the direction normal to the surface. The primary advantage of using such an adaptive algorithm for prisms is that the data structures needed for its implementation are essentially as simple as that for refining a 2-D triangular grid.

The directional division of the prisms does not increase resolution of flow features that are aligned in a direction that is normal to the wall surface. However, a grid redistribution algorithm can be employed in order to recluster nodes in the normal direction so as to better resolve the viscous stresses [1, 8].

The tetrahedral cells constitute the portion of grid where inviscid flow features are dominant. These features do not exhibit the directionality that is generally prevalent in viscous stresses. Hence, the tetrahedra are refined by division into eight, four, or two subcells.

Redistribution of Prisms

The redistribution algorithm increases local grid resolution by clustering existing grid points in regions of interest. A measure of the grid resolution required normal to the *no-slip* wall is the values

of $y^+ = \frac{u_\tau y}{\nu}$, with $u_\tau = \sqrt{\frac{|\tau_{wall}|}{\rho_{wall}}}$ being the wall friction velocity. A criterion based on the values of y^+ at the wall is employed to either *attract* nodes towards the wall or *repel* them away from the surface so that a specific value of y^+ is attained at all the wall nodes. This procedure in essence determines a new value for the spacing δ_{wall} of the first node off the wall at all locations on the wall surface. The nodes in the prismatic region are then reclustered along the marching lines emanating from the corresponding wall node, in accordance with the new value of δ_{wall}. Details are presented in [2].

Application of the Adaptation Method

The test case of flow past a sphere at a free stream Mach number of $M_\infty = 1.4$ and a Reynolds number of $Re = 1000$ (based on the radius of sphere) is considered. The flow is characterized by both inviscid and viscous flow features such as shock waves and boundary layer separation. Details are given in [2].

The hybrid grid adaptation algorithm developed in the present work is now implemented to obtain numerical solution for the same flow situation discussed above. A coarse hybrid grid comprising $\sim$ *1400* wall boundary nodes and $\sim$ *100K* tetrahedra is used as the initial grid. The prismatic region is constituted by *20* layers of prisms. The locally adapted grid obtained after h-refinement based on an initial solution is shown in Figure 6. The figure shows the tessellation on the wall surface, on the symmetry plane as well as on an equatorial plane cutting through the interior of the grid, normal to the symmetry plane. It is clearly seen that embedding in the tetrahedral region is focussed near the shock location just outside of the prismatic-tetrahedral interface. The prismatic region is also directionally refined near the upstream and downstream sections of the body. This is due to the flow upstream accelerating rapidly from the upstream stagnation point and the flow downstream separating that causes flow gradients in the lateral directions that are detected by the directional adaptive algorithm. The embedded hybrid grid comprises $\sim$ *2500* wall boundary nodes and $\sim$ *275K* tetrahedra. Mach number contour lines of the solution obtained on the adapted grid are shown in Figure 7.

The effect of grid redistribution in the viscous region is next shown by selecting an initial grid that has a relatively large wall spacing δ_w and further, the prism layers are equispaced as shown in Figure 8 (a). The grid has $\sim$ *1400* wall nodes and $\sim$ *100K* tetrahedra. Based on an initial solution obtained on this grid, the redistribution algorithm is used to recompute the values of δ_w at all the wall boundary nodes, using y^+ as the detection parameter. The hybrid grid with the redistributed prismatic region is shown in Figure 8 (b). Observing the grid in the fore section, it is seen that the redistribution algorithm reclusters the grid substantially by attracting the nodes very close to the wall in order to resolve the large gradients in the normal direction. In the aft region, the boundary layer thickens substantially and separates and the algorithm is seen to push the nodes away from the wall.

Acknowledgments

This work was supported by NASA Grant NAG1-1459, the NSF Grant ASC-9357677 (NYI Program), and the Texas Advanced Technology Program (ATP) Grant # 003658-413. We would

like to thank Ms. Karen Bibb of NASA Langley for giving us access to the FELISA mesh generation code. Supercomputing time was provided by the NAS Division of the NASA Ames Research Center.

References

[1] Y. Kallinderis and S. Ward, "Prismatic Grid Generation for 3-D Complex Geometries", *Journal of the American Institute of Aeronautics and Astronautics*, Vol. 31, No. 10, pp. 1850-1856, October 1993.

[2] V. Parthasarathy, Y. Kallinderis, and K. Nakajima, "A Hybrid Adaptation Method and Directional Viscous Multigrid with Prismatic/Tetrahedral Meshes," AIAA Paper 95-0670, Reno, NV, January 1995.

[3] J. Peraire, J. Peiro, L. Formaggia, K. Morgan and O.C. Zienkiewicz, "Finite Element Euler Computations in Three Dimensions," *AIAA 26th Aerospace Sciences Meeting*, Reno, AIAA Paper 88-0032, January 1988

[4] J. Peiro, J. Peraire, and K. Morgan, "FELISA System Reference Manual", 1994.

[5] J. Bonet, and J. Peraire, "An Alternating Digital Tree (ADT) Algorithm for Geometric Searching and Intersection Problems", Int. J. Num. Meth. Eng., Vol. 31, No. 1, 1990.

[6] Y. Kallinderis and P. Vijayan, "An Adaptive Refinement Coarsening Scheme for 3-D Unstructured Meshes", AIAA Journal, Vol 31, No.8, pp 1440-1447, Aug. 1993.

[7] S. Ward and Y. Kallinderis, "Hybrid Prismatic/Tetrahedral Grid Generation for Complex 3-D Geometries", AIAA Paper 93-0669, Reno, NV, January 1993.

[8] Y. Kallinderis, A. Khawaja, and H. McMorris "Hybrid Prismatic / Tetrahedral Grid Generation for Complex Geometries", AIAA Paper 95-0211, Reno, NV, January 1995.

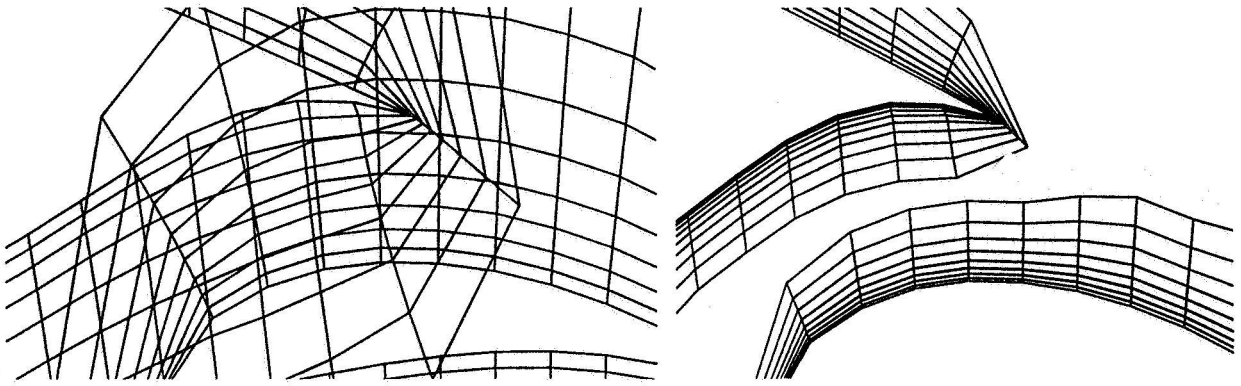

Figure 2: (a) Prismatic grids grow around each body independently of one another (b) Mutual receding of the two prismatic grids removes prior overlapping (view on the symmetry plane).

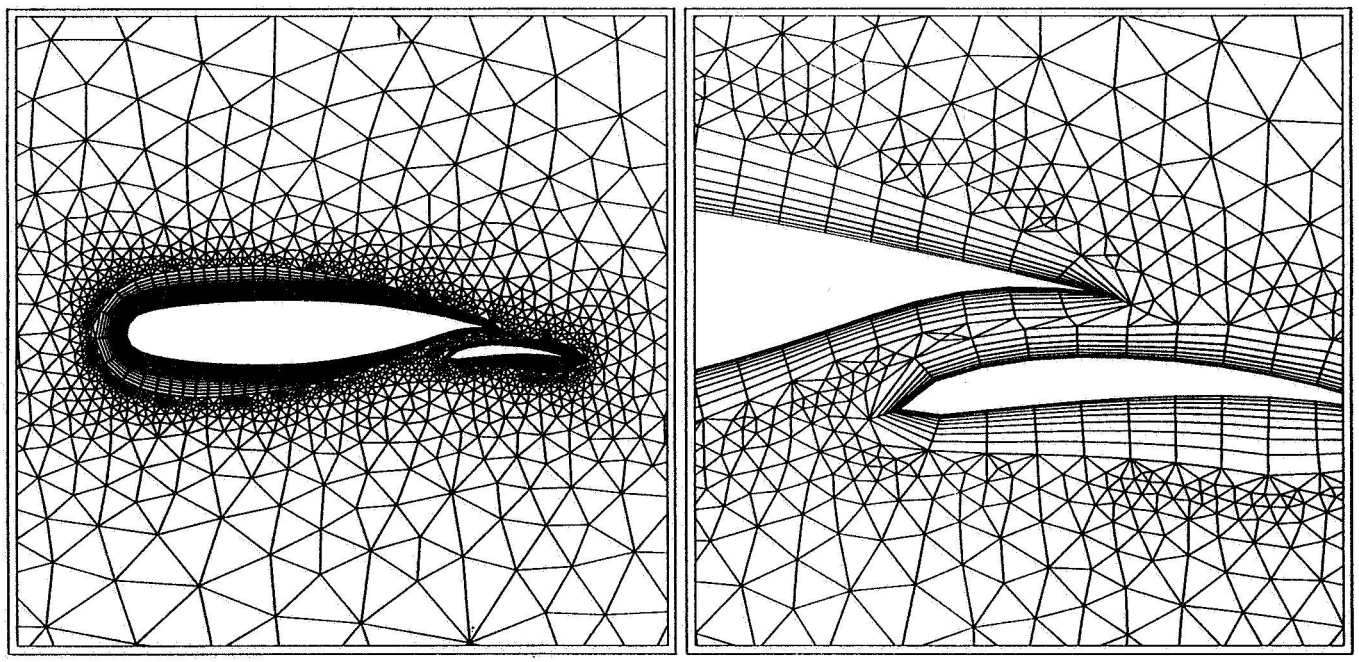

Figure 3: (a) Tetrahedral grid fills the areas in between the two prismatic meshes (b) Enlarged view of the gap region between the two bodies (view on the symmetry plane).

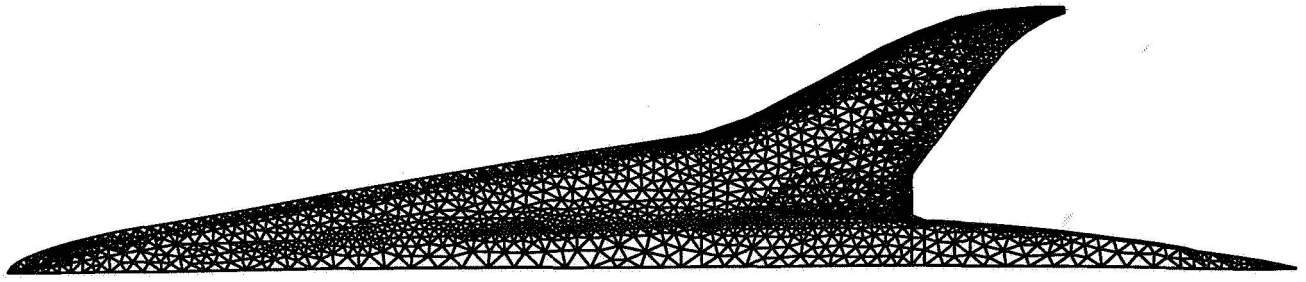

Figure 4: Triangulation of the HSCT surface (4412 triangles, 2275 nodes)

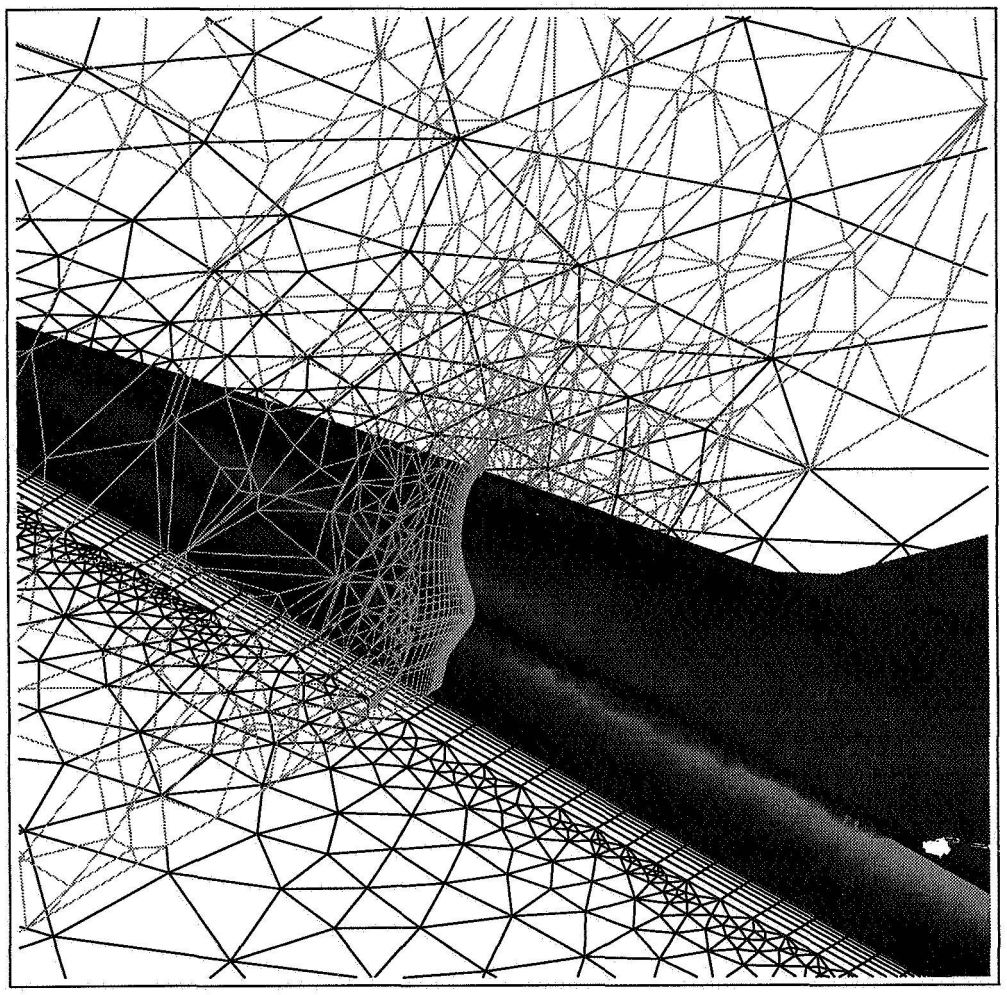

Figure 5: View of the hybrid mesh around the HSCT on two different planes that are perpendicular to each other. The first plane is the symmetry (dark lines), while the second is intersecting the fuselage at a location upstream of the wing (light lines).

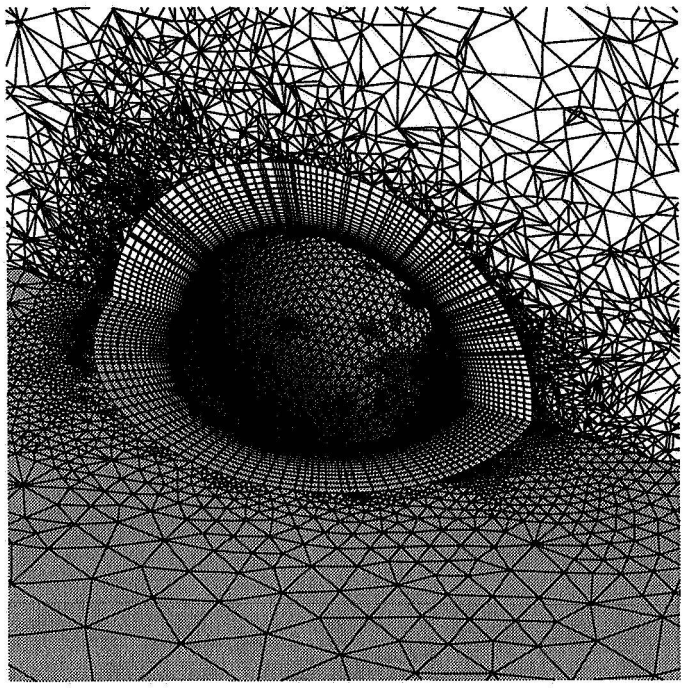

Figure 6: An isometric view of the tessellation on the wall surface, symmetry plane and an interior equatorial plane. Hybrid grid embedded isotropically in the tetrahedral region and directionally in the prismatic region.

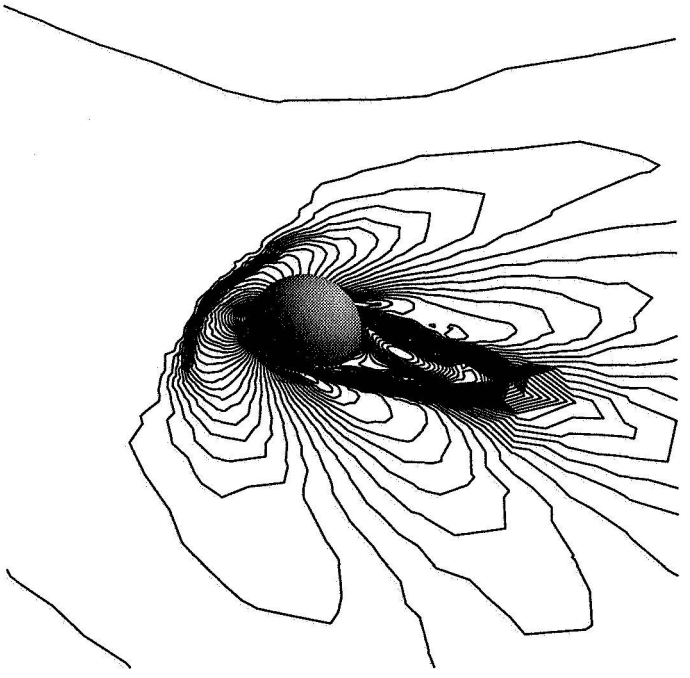

Figure 7: Mach number contour lines of the solution on the symmetry plane. Solution obtained using an embedded hybrid grid ($M_{min} = 0., M_{max} = 2., \Delta M = 0.05$).

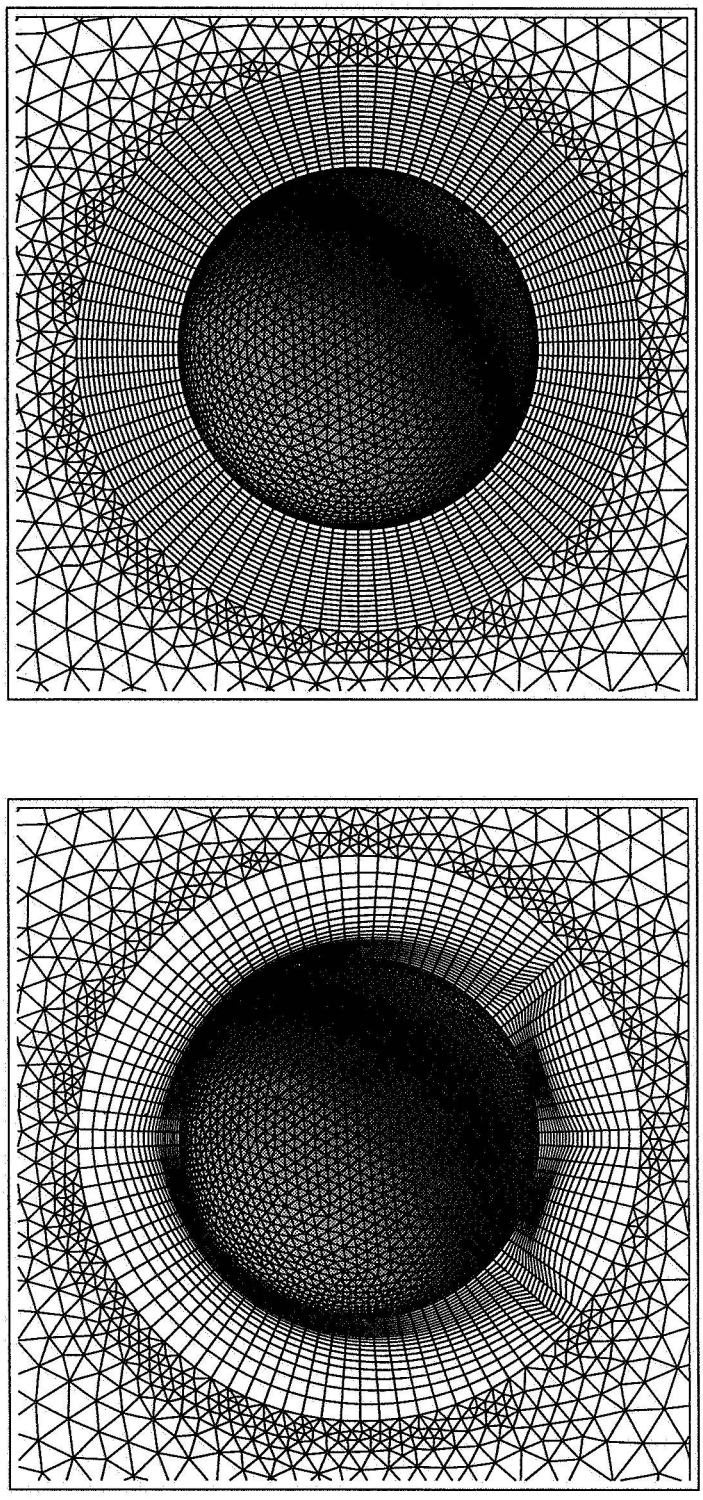

Figure 8: Tessellation on the symmetry plane showing the clustering of grid points in the prismatic region for (a) an initial grid with equispaced prismatic layers and (b) the grid obtained after redistributing the former.